Research Article J. Electrochem. Sci. Technol., 2017, 8(3), 236-243

Journal of Electrochemical Science and Technology
jecst.org

A Newly Designed Fixed Bed Redox Flow Battery Based on Zinc/Nickel System

Safe ELdeen M.E. Mahmoud[1]*, Yehia M. Youssef[2], I. Hassan[1], and Shaaban A. Nosier[3]

[1]*Basic and Applied Science Department, College of Engineering and Technology, Arab Academy For Science And Technology And Maritime Transport, Alexandria, Egypt*

[2]*Department of Industrial Engineering, College of Engineering and Technology, Arab Academy For Science And Technology And Maritime Transport, Alexandria, Egypt*

[3]*Department of Chemical Engineering, Faculty of Engineering, Alexandria University, Alexandria, Egypt*

ABSTRACT

A fixed-bed zinc/nickel redox flow battery (RFB) is designed and developed. The proposed cell has been established in the form of a fixed bed RFB. The zinc electrode is immersed in an aqueous NaOH solution (anolyte solution) and the nickel electrode is immersed in the catholyte solution which is a mixture of potassium ferrocyanide, potassium ferricyanide and sodium hydroxide as the supporting electrolyte. In the present work, the electrode area has been maximized to 1500 cm^2 to enforce an increase in the energy efficiency up to 77.02% at a current density 0.06 mA/cm^2 using a flow rate 35 cm^3/s, a concentration of the anolyte solution is 1.5 mol L^{-1} NaOH and the catholyte solution is 1.5 mol L^{-1} NaOH as a supporting electrolyte mixed with 0.2 mol L^{-1} equimolar of potassium ferrocyanide and potassium ferricyanide. The outlined results from this study are described on the basis of battery performance with respect to the current density, velocity in different electrolytes conditions, energy efficiency, voltage efficiency and power of the battery.

Keywords : Fixed bed, Redox flow battery, Energy storage, Zinc/nickel RFB, Cost analysis

Received : 23 April 2017, Accepted : 20 July 2017

1. Introduction

Nowadays there is a worldwide concern and interest in the production of renewable energy as well as carbon-free systems such as wind energy and solar energy in order to find out a solution for the CO_2 emissions and reduce its impact on the environment. These renewable energies can produce a great amount of energy sources to meet the worldwide needs. However, the challenge which is facing these renewable energy means is how to store them [1]. One of the highly impressive solutions for stationary energy storage is the electrochemical systems such as the redox flow batteries (RFBs). This system is well characterized as one of the recent technology with an excellent promising choice for energy storage [2]. The redox flow batteries can be used in remote areas to store energy. They can work along with the solar photovoltaic arrays and wind turbine farms as well. They can also supply electric energy when the traditional power generation systems do not provide sufficient quantities. The main advantages of the RFBs are their flexibility in design, reliability, acceptable process, and their low costs [3].

Among various types of redox flow batteries are Fe/Cr, Zn/Br, V/Br with the most successful RFB is the vanadium one. The advantage of using VFBs is that the type of metal used for both electrolytes is identical. Moreover, there is no decreasing in its storage capacity with time, but some differences in the oxidation state of the metal ion charge at the two electrodes exist. Therefore, vanadium in the tetravalent and pentavalent forms are used on one side and

*E-mail address: safeeldeenelsayed@yahoo.com

DOI: https://doi.org/10.5229/JECST.2017.8.3.236

vanadium divalent and trivalent are placed on the other side [4].

The zinc/bromine redox flow battery is another model of these systems. It contains two electrolytes each one is stored in external tanks and circulated through the electrochemical cell. At the negative electrode the zinc ions are dissolved in the aqueous phase and back and at the positive electrode, the bromide ions are changed to be bromine and back. The bromide ions can combine with bromine molecules to produce the tribromide ion which occurs mainly in the liquid bromine. Due to the high toxicity of the produced bromine, it is preferred to use a complexing agent. To avoid self-discharge, there is a separator (ion selective membrane) between the two electrolytes which prevent the combination of both zinc and bromine and allow the passage of H^+ ions. Despite the high cell voltage and low materials cost, this cell has a limited usage due to the corrosion of its materials and the low energy densities and its short life cycle [5-9].

The iron/chromium redox flow battery is one of the first studied flow battery technologies by National Aeronautics and Space Administration (NASA). The anolyte solution in this battery is an aqueous solution of ferric-ferrous redox couple, while the catholyte solution is a chromous and chromic couple and both are mixed with hydrochloric acid. An ion selective membrane is placed between the anodic and cathodic half-cells to separate the two electrolytes and to allow the passage of H^+ ions. However, some of these systems are not strictly redox flow batteries because their half-cell reactions involve the deposition of solid species [10-13]. Among all the aqueous RFB systems, zinc/cerium redox flow battery consists of Zn/Zn^{2+} and $Ce^{3+/}Ce^{4+}$ redox couples. This cell shows a high cell capacity and power which can result from a higher cell voltage under a certain concentration of electrolyte [14-16].

The present study is aimed to present zinc/nickel redox flow battery as a rechargeable battery where the zinc is used as an anode inside the cell during discharging and the inert electrode (nickel) is placed inside the cell as a cathode during the discharging. The anolyte solution is sodium hydroxide solution while the catholyte solution is an equimolar concentration of potassium ferrocyanide and potassium fericyanide and mixed with sodium hydroxide solution as a supporting electrolyte. The Zinc is connected to the negative terminal of the direct current power supply to produce the reduction reaction. On the other hand, nickel is connected to the positive terminal of the direct current power supply to produce the oxidation reaction [17]. The galvanic cell is operated during discharging where the zinc acts as anode and oxidized to be zinc ions and the nickel acts as the cathode where the ferric ions are reduced on the nickel electrode surface to be ferrous ions during the discharging process.

2. Experimental

2.1 Materials

The catholyte solution is an equimolar solution of potassium ferricyanide (0.1 mol L^{-1}, 0.2 mol L^{-1} and 0.3 mol L^{-1}) and potassium ferrocyanide (1.0 mol L^{-1}, 1.5 mol L^{-1} and 2.0 mol L^{-1}). Sodium hydroxide is used as a supporting electrolyte, while the anolyte solution (1.0 mol L^{-1}, 1.5 mol L^{-1} and 2.0 mol L^{-1}). The above solutions were prepared using distilled water.

2.2 Measures and analysis

The experiments were performed by using the following illustrated systems in Figs. 1 and 2. The apparatus used in Fig. 1 consists of a fixed bed electrochemical reactor, flowing circuit and an electrical circuit. The reactor consists of two cubic compartments made of plexiglass ($7\times7\times7$ cm^3). In addition, the reactor is divided into three sections: inlet and outlet sections, while the working section is represented in Fig. 2. The inlet and outlet sections consist of two plastic pipes with two plastic valves for each section to control the flow rate. While the working section consists of two cubic compartments which are separated by anion exchange membrane (Fumasep FAA-3-PK-130) which allows the passage of the hydroxide ions only and prevents the positive ions from passing between the two half cells. The anodic compartment consists of a sheet of zinc metal (6.5×6.5 cm) and zinc cylinders (0.9 cm height × 0.9 cm diameter) with aspect ratio 1:1 connected to each other to act as anode immersed in different concentrations of sodium hydroxide solution. The cathode compartment consists of a nickel sheet (6.5×6.5 cm) and nickel cylinders (0.9 cm (height) × 0.9 cm (diameter)) with aspect ratio 1:1 connected to each other and are immersed in equimolar concentration of potas-

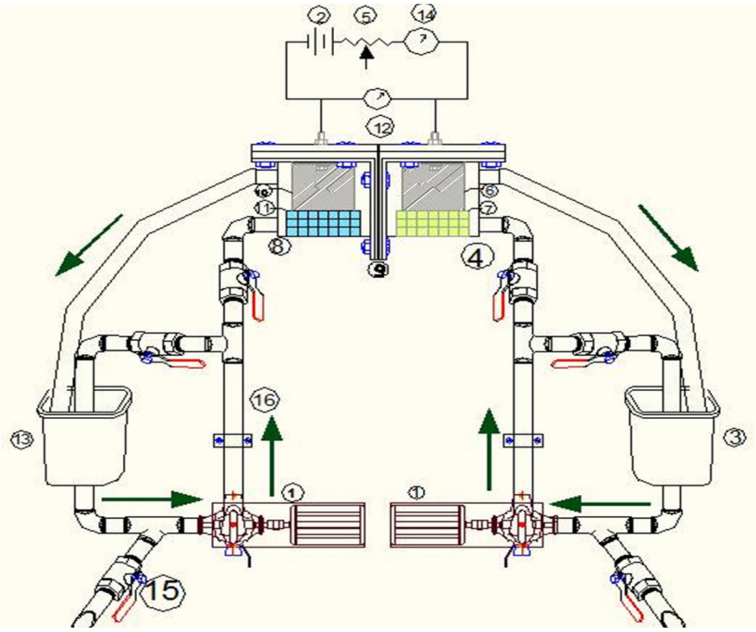

1. Iwaki plastic centrifugal pumps.
2. D.C power supply.
3. Plastic reservoir for catholyte solution.
4. Cubic compartments of pexiglass for the cathodic electrolyte.
5. Variable resistance.
6. Nickel metal electrode (6.5 x 6.5 cm).
7. Nickel cylinders electrodes (0.9 cm x 0.9 cm).
8. Cubic compartment of plexiglass for the anodic electrolyte.
9. Anion exchange membrane (Fumasep FAA-3-PK-130).
10. Zinc metal electrode (6.5 x 6.5).
11. Zinc cylinder electrodes (0.9cm (height) * 0.9cm (diameter)).
12. Voltammeter.
13. Plastic reservoir for the anolyte solution.
14. Ammeter.
15. Plastic valve.
16. Plastic pipeline

Fig. 1. Schematic diagram and major components of zinc/nickel fixed bed redox flow battery.

sium ferricyanide and potassium ferrocyanide in sodium hydroxide as supporting electrolyte. The solution is pumped from the storage tanks to the two half cells using Iwaki plastic centrifugal pumps with half horsepower.

The electrical circuit consisted of a 12-volt direct current power supply, a multirange ammeter connected in series with the cell and a high impedance voltmeter is connected in parallel with the circuit to measure the cell voltage. Before each run, the solution is circulated between the plastic storage tank and the two half-cells using a plastic centrifugal pump.

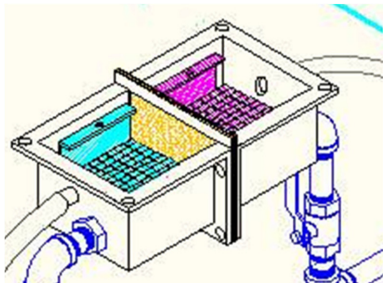

Fig. 2. Isometric drawing for zinc/nickel electrodes in the two half cells of RFB and the ion exchange membrane separates two compartments.

The solution entered the half-cell through the inlet tube placed above the bottom of the cell. A similar outlet tube was placed at the top of the reactor. The solution flow rate is controlled by bypass valves. The charging voltage and current were measured versus time during reduction of zinc metal in sodium hydroxide solution and cathodic oxidation of ferrous ions to ferric ions on the nickel surface. The discharging voltage and current are measured versus time during oxidation of zinc ions in sodium hydroxide solution and reduction of ferric ions to ferrous ions on the nickel surface.

3. Results and Discussion

3.1 Charge / discharge performance

As shown in Figs. 3, 4 and 5, one can conclude during charging that the voltage increases in the first 10 min then becomes constant. In addition, the discharging voltage decreases gradually in the first 10 min of discharging then becomes constant at different current densities. It is also evident that the voltage efficiency decreases with increasing the current owing to maintaining the columbic efficiency constant at 100%. At high current densities, the mass transfer processes are unable to supply the electro active ions to the electrode surface at the needed rate to keep the reaction going and this raises the limiting current. The electrode potential is thus shifted to more negative or more positive values, leading to the breakdown of water and gassing side reactions that produce hydrogen and oxygen at the negative and positive electrodes respectively during charging. Moreover, the magnitude of the limiting current is a function of the concentration of electro active ions in solution [18]. Moreover, the current density was identified to decrease, the voltage

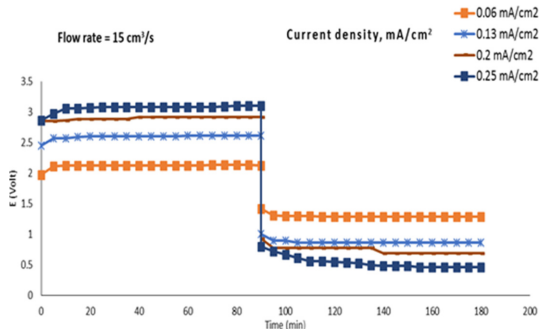

Fig. 3. Effect of time versus charging and discharging voltage at different current densities (Catholyte concentration = 0.1 mol L^{-1} Fe^{2+}/Fe^{3+} and 1.0 mol L^{-1} NaOH and anolyte concentration = 1.0 mol L^{-1} NaOH).

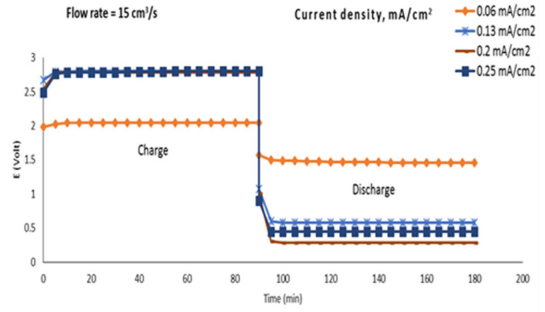

Fig. 4. Effect of time versus charging and discharging voltage at different current densities. (Catholyte concentration = 0.2 mol L^{-1} Fe^{2+}/Fe^{3+} and 1.5 mol L^{-1} NaOH and anolyte concentration = 1.5 mol L^{-1} NaOH).

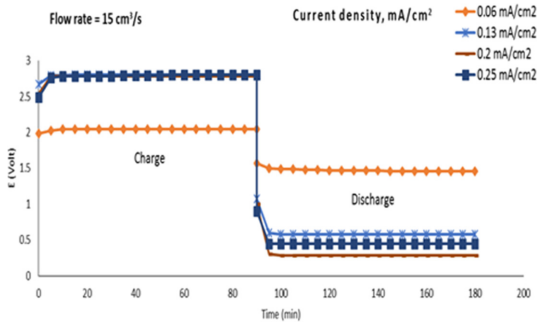

Fig. 5. Effect of time versus charging and discharging voltage at different current densities. (Catholyte concentration = 0.3 mol L^{-1} Fe^{2+}/Fe^{3+} and 2.0 mol L^{-1} NaOH and anolyte concentration = 2.0 mol L^{-1} NaOH).

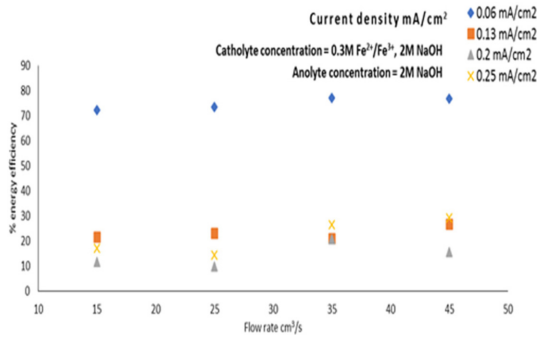

Fig. 6. Effect of flow rate versus % of the energy efficiency.

dropped between the charging and the discharging voltage decreased based on the given data in Figs. 3, 4 and 5.

3.2 Effect of flow rate

As shown in the Fig. 6, the energy efficiency increases with increasing the flow rate of the electrolyte solution. Increasing the rate of mass transfer (increasing the flow rate) of the ions to the electrode surface, by either stirring or by pumping the solutions at higher velocities through each half-cell at a faster rate which decreases the thickness of the diffusion layer or boundary layer. It is also evident that the energy efficiency decreases with increasing the current density due to the increase in the resistance or load. And also the concentration polarization will lead to gassing side reactions if the current density exceeds the limiting current for the cell charging reactions. When this occurs, the cell can often go into overcharge, which is highly undesirable since this can potentially lead to the formation of hydrogen gas at the negative electrode. Where the electrodes are used in the cell, gassing side reactions occurs during overcharge [18].

3.3 Effect of current density on the Energy efficiency and the voltage efficiency

The overall energy efficiency of the cell is a measure of the amount of actual energy released on discharge relative to the amount of energy required to charge the cell. It is generally calculated according to the following expression (1) [18]. In addition, the energy efficiency is calculated from the product of the coulombic and voltage efficiencies as expressed in equation (2).

$$\eta_e = \oint \frac{Id * Vd}{Ic * Vc} dt * 100\% \quad (1)$$

where η_e is the overall energy efficiency (%), I_d is the cell current during discharge (A), V_d is the cell voltage during discharge (V), I_c is the cell current during charge (A) and V_c is the cell voltage during charge (V).

$$\eta_e = (\eta c * \eta v) \quad (2)$$

where η_e is the energy efficiency (%), η_c is the coulombic efficiency (%) and η_v is the voltage efficiency (%).

Generally, the energy efficiency is an indicator of the overall cell performance and reflects the combined trends in coulombic and voltage efficiencies as a function of current density. The combined effect on the overall energy efficiency is an optimal operating current density for maximum energy efficiency. Although other factors including capital and maintenance costs could shift the optimal current density to higher values in practice. But in the present work, the coulombic efficiency is considered to be 100% owing

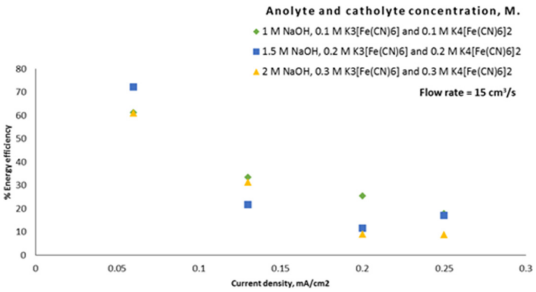

Fig.7. Effect of current density on the energy efficiency.

Table 1. Energy efficiency of different redox types.

Type of redox types	Current density (mA/cm^2)	Max Energy efficiency (%)	Current efficiency (%)
Nickel-cadmium	5-15	60	80
Nickel-metal hydride	5-10	50	85
Iron-Chromium	9	81	81
Bromine-Polysulfide	600	75	90
Vanadium-Vanadium	800	73	98
Soluble lead acid	100-600	82	85
Zinc-Nickel sheet	3.3-11.3	60.64	100
Present work	0.06-0.25	77.02	100

to the same current density during charging and discharging and this means that the energy efficiency equals to the voltage efficiency. In other words, the overall cell performance depends on the voltage efficiency as expressed by equation (3) [18].

$$\eta_e = \eta_v \quad (3)$$

As represented in Fig. 7, the loss of cell energy increases with increasing the current and therefore, the energy efficiency decreases with increasing current density. Table 1 list out the energy efficiencies of different redox types [18].

$$P = I*V \quad (4)$$

P = Power, I = current density, V = Voltage

To minimize the resistance and power loss, the membrane must have a high ionic conductivity, and hydrophilic characters at the interface between the liquid electrolyte and solid membrane surface to ensure a fast ion transfer. In addition, the fast ionic transport must be highly selective and the transport of active species must be minimized to reduce capacity and energy losses. The power is also affected by the shunt current and as the flow rate and concentration of solution increase, the pressure drop increases and may lead to enlargement in the power loss in the pumping system. As shown in Fig. 8, the power consumed during charging increases as the flow rate increases and this behavior means that the power loss increases. However, the pumping of solutions at higher velocities through each half-cell at a faster rate will increase the limiting current and the concentration polarization will lead to gassing side reactions. If the current density exceeds the limiting current for the cell charging reactions, the cell can often go into overcharge, which is highly undesirable since this can potentially lead to the formation of hydrogen gas at the negative electrode [18]. As shown in Fig. 9, the power generated during discharging decreases as the current density increases and this situation means that the power loss increases to overcome the overcharge in the concentration polarization.

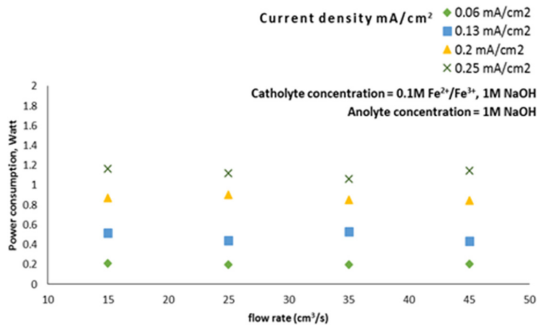

Fig. 8. Effect of Flow rate on the power of charging current density.

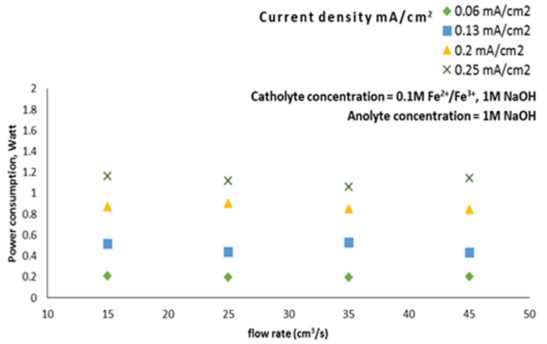

Fig. 9. Effect of Flow rate on the power of discharging current density.

Table 2. Comparison of electrode sheet Zinc-Nickel RFB and fixed bed Zinc-Nickel fixed bed RFB.

RFB	Current density (mA/cm^2)	Electrode area (cm^2)	Power consumed during charging (watt)	Power generated during discharging (watt)
Zinc-Nickel RFB	3.3	150	2.3-2.9	1.3-1.5
	7		2.5-3	0.9-1.3
	11.3		4-5.5	0.4-1.1
Zinc-Nickel fixed bed RFB	0.06	1500	0.10-0.27	0.05-0.15
	0.13		0.43-0.67	0.04-0.25
	0.20		0.78-1.018	0.04-0.2
	0.25		1.03-1.49	0.05-0.304

Table 3. Comparison of costs for the proposed zinc/nickel versus other RFBs all vanadium RFBs.

Specification	All vanadium redox flow battery	Zinc / Nickel fixed bed redox flow battery (Present work)
Current density	52 mA/cm^2	0.16 mA/cm^2
Number of stacks	10	1
Electrode area	1.75 m^2	0.15 m^2
Frame + Components	$1218	$600
Ion exchange membrane	$165	$165
Electrolyte tanks	$510	$20
Pumps	$448	$450
Control system	$700	$20
Chemicals	V_2O_5 $756/kg	($15/ 1kg Sodium hydroxide, $100/ 1 kg Potassium ferrocyanide, $100/ 1 kg Potassium ferricyanide)
Total costs	$4665	$1167

3.4 Cost Analysis

The commercial development and current economic incentives associated with energy storage using redox flow batteries (RFBs) are summarized in this analysis section as listed in Table 3. The analysis is mainly focused on making a comparison between all vanadium redox flow battery and the zinc/nickel fixed bed redox flow battery as illustrated in the present work. The potential benefits of increasing battery based energy storage for electricity grid load leveling and MW-scale wind/solar photovoltaic-based power generation are now being realized at an increasing level. Commercial systems are being applied to distribution systems utilizing kW scale renewable energy flows [19].

4. Conclusions

Based on the outlined data in the present study, several important points can be concluded and listed out. The power consumed during charging increases as the flow rate increases and this means that the power loss increases, due to pumping the solutions at higher velocities through each half-cell at a faster rate, which increases the limiting current. The concentration polarization may lead to gassing side reactions when the current density exceeds the limiting current during the charging reactions. This will cause the overcharge of the cell, which is highly undesirable. However, the overcharge can potentially lead to the formation of hydrogen gas at the negative electrode. The power generated during discharging decreases as the flow rate increases and this means that the power loss increases. All cell losses increase with increasing current density so that the energy efficiency and the voltage efficiency decrease. Finally, the total costs for establishing Zn/Ni fixed bed RFBs is lower than the total costs for establishing All vanadium RFBs.

The results of this study may be extended to explore further evaluation points according to the following recommendations. (i) Change the shape of the electrode to a hollow cylinder. (ii) Use a vibrated electrode. (iii) Use multiple stacks to increase power density and energy efficiency. (iv) Change the surface area of the electrode. (v) Change the electrolyte volume in the tank. (vi) Lower the temperature inside the stack or the cell to decrease the ohmic resistance by using the cooling jacket for both the anolyte and catholyte solutions.

References

[1] P. Alotto, M. Guarnieri, F. Moro, A review, *Renew. Sustain. Energy Rev.*, **2014,** *29* 325-335.
[2] Q. Xu and T. S. Zhao, *Prog. Energy Combust. Sci.*, **2015**, *49*, 40-58.
[3] K. Yesol, C. Seho, P. Se-Kook, J. Jae-Deok, L. Young-Seak, *Appl. Chem. Eng.,* **2014**, *25(3),* 292-299.
[4] H. Prifti, A. Parasuraman, S. Winardi, T. M. Lim, and M. Skyllas-kazacos, *Membr.* **2012,** *2*, 275-306.
[5] A.Z. Weber, M.M. Mench, J.P. Meyers, P.N. Ross, J.T. Gostick, Q. Liu, *J. Appl. Electrochem.*, **2011**, *41(10)*,

1137-1164.
[6] J.H. Yang, H.S. Yang, H.W. Ra, J. Shim, J. D. Jeon, *J. Power Sour.*, **2015,** *275*, 294-297.
[7] T.I. Evans, R.E. White, *J. Electrochem. Soc.*, **1987**, *134(4)*, 866-874.
[8] M. Hromadova, W.R. Fawcett, *J. Phys. Chem*. A, **2001**, *105(1),* 104-111.
[9] H.S. Lim, A.M. Lackner, R.C. Knechtli, *J. Electrochem. Soc.,* **1977**, *124(8)*,1154-1157.
[10] L.Swette, V. Jalan, NASA CR-174724, DOE/NASA/ 0262e271, **1984**.
[11] C.P. de Leon, A. Frias-Ferrer, J. Gonzalez, D.A. Szanto, F.C.Walsh*, J Power Sour.*, **2006,** *160(1),* 716-732.
[12] Wu, H., J. R. Selman, P. Hollandsworth, *Indian J. Technol*, **1986**, *24(7)*, 372-380.
[13] Y.K. Zeng, X.L. Zhou, L. An, L. Wei, T. S. Zhao, *J. Power Sour.*, **2016**, *324*, 738-744.
[14] Z.P. Xie, D.B. Zhou, F.J. Xiong, S.M. Zhang, K.L. Huang, *J. Rare. Earths*, **2011**, *29(6),* 567-573.
[15] G. Nikiforidis, L. Berlouis, D. Hall, D. Hodgson, *J. Power Sour.* **2012**, *206*, 497-503.
[16] Z. Xie, Q. Liu, Z. Chang, and X. Zhang, *Electrochim. Acta*, **2013**, *90*, 695-704.
[17] M.M. Ibrahim, I.H. Mohamed, Y. Youssef, *13th International Conference on Clean Energy (ICCE-2014)* **2014**, 312-321.
[18] M. Skyllas-Kazacos, C. Menictas, T. Lim, Woodhead Publishing Limited, **2013**.
[19] C.P. de Leon, A.F. Ferrer, J. Power Sour, **2006**, *160(1)*, 716-732.